Journal of Basic Sciences and Artificial Intelligence (JBSAI)

DOI: 10.65098/jbsai.01.2026.37.45

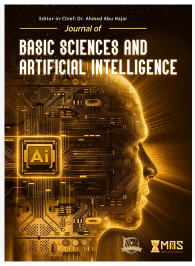

RESEARCH ARTICLE

Dynamic Performance and Torque Optimization of a Bio-Inspired Tadpole-Like Flexible Underwater Robot: A Comparative Study of SMC, Type-1, and Interval Type-2 Fuzzy Controllers

Abdul Fattah Jamali*, **Hassan Al-Naddaf, Bassem Fares**

Department of Control and Automation Engineering, Faculty of Electrical and Electronics Engineering, University of Aleppo, Aleppo 12212, Syria
****Corresponding Author Email: jamali@al-shamal.edu.sy***

ARTICLE DETAILS

Article History:

Received: 05 July 2026
Accepted: 25 Aug 2026
Available online: 30 Aug 2026

Online Article Code

ABSTRACT

Mimicry of underwater robots with high agility capabilities, such as tadpole-like locomotion, provides high propulsion efficiency. But the incorporation of a flexible and under-actuated tail structure into these robots results in complicated and highly nonlinear dynamics that are hard to control in various aquatic environments. This paper provides a complete dynamical study and quantitative comparison among three different robust control systems: traditional sliding mode control (SMC), type-1 fuzzy SMC (Type-1 FSMC), and interval type-2 fuzzy SMC (IT2-FSMC), used on a dual-motor tadpole-like flexible underwater robot. The main aim of this research is to study the control effort (torque) and trajectory tracking performance under multi-gradient operating situations ranging from nominal (0%) to parametrically extreme (50%) disturbances affecting individual physical parameters. From numerical simulation studies incorporating realistic hardware constraints, it can be seen that although the conventional SMC and Type-1 FSMC perform reasonably well at 0% uncertainty, they become dynamically unstable with high-frequency chattering effects at severe uncertainty levels. In contrast, the innovative IT2-FSMC model, which utilizes the concept of Footprint of Uncertainty along with the highly efficient Nie-Tan type reduction scheme, successfully copes with severe multi-parameter coupled disturbances. The IT2-FSMC is capable of producing an extremely smooth and chattering-free torque control signal, optimizing computational efficiency for embedded applications.

KEYWORDS

Bio-Inspired Underwater Robot, Tadpole-Like Locomotion, Interval Type-2 Fuzzy Sliding Mode Control, Torque Optimization, Parametric Uncertainty, Chattering Suppression, Flexible-Structure Dynamics

1. INTRODUCTION

In the quickly evolving area of marine engineering and undersea exploration, AUVs must be designed to perform increasingly sophisticated functions in extremely unpredictable surroundings. Conventional underwater robots, mainly having stiff and bulky structures, have several constraints related to their energy usage, drag, and agility. Scientists thus took inspiration from nature and developed bio-inspired underwater robots that address these limitations. Particularly, the robot design based on the highly agile and efficient movement of the tadpole (or sub-carangiform fish) is highly beneficial in terms of propelling itself in water with high efficacy. Through a flexible tail section powered by a dual-motor joint drive system, the bio-inspired robot can easily maneuver itself in water with high efficiency. The integration of such advanced robotic systems aligns with recent cutting-edge developments in complex operational environments, such as orbital angular momentum beamforming for index modulation, long-distance non-orthogonal transmission capacity evaluation, high-precision object detection under hybrid cloud-fog architectures, and high-precision deep-sea geomagnetic data sampling with compressive sensing (Yu et al., 2014; Katzschmann et al., 2018; Wen et al., 2012; Wang et al., 2019).

Nonetheless, going from inflexible mechanical structures to a bio-inspired flexible one raises many challenges for mathematical modeling and control designs. Dynamics-wise, an example of a robotic underwater system that resembles a tadpole with a flexible tail is a highly nonlinear, strongly coupled, and underactuated mechanical system. The reason for underactuation lies in the infinite number of degrees of freedom for elastic vibration of the tail, which do not have dedicated actuators. Hence, a joint actuator system composed of two motors has to ensure at the same time tracking of the desired rigid body motion as well as providing active damping of elastic vibrations of the tail. Such a task becomes even harder because of harsh conditions of the marine environment, which imply constant presence of external perturbations, changing ocean currents, dry friction in joints, and changing hydrodynamic characteristics, for example, the added mass matrix.

For such dynamics and perturbations to be efficiently handled, the classic sliding mode control (SMC) technique has usually been used as a benchmark solution owing to its complete immunity from matched uncertainties. Nonetheless, the application of SMC is limited by the frequent switching nature of the control input, which introduces an undesirable phenomenon called chattering. For applications of flexible structures, the chattering effect becomes extremely dangerous because it causes resonant excitation of the system through high-frequency energy injection to the unmodeled structural modes, resulting in control spillover that leads to total dynamic instability and fatigue of the joint motors.

In order to overcome the chattering problem without losing robustness, Type-1 Fuzzy Sliding Mode Control (Type-1 FSMC) has been developed. By using the continuous fuzzy inference system instead of the discontinuous signum function, Type-1 FSMC effectively solves the chattering problem. However, it exhibits poor results when working in the presence of extreme parametric perturbations (more than 0% uncertainty). Type-1 FSMC uses crisp membership functions; it does not have enough mathematical flexibility to capture the huge number of linguistic and parametric errors. Thus, when uncertainties become excessively high (for instance, 50% deviation from the nominal values), the Type-1 FSMC suffers from dynamic breakdown, causing incorrect torque signals and tracking errors without any compensation.

In order to solve this key drawback, this paper presents an innovative hybrid nonlinear control approach based on the Interval Type-2 Fuzzy Sliding Mode Control (IT2-FSMC). IT2-FSMC incorporates the "Footprint of Uncertainty" (FOU) into the control system owing to its upper and lower membership functions, giving an additional degree of mathematical flexibility to the controller. With the help of the iterative Karnik-Mendel type-reduction approach, the IT2-FSMC can easily absorb the large amount of uncertainties that completely paralyze conventional controllers.

The novelty of this paper is the dynamical comparison between the traditional SMC, Type-1 FSMC, and the novel IT2-FSMC for the biologically inspired tadpole-like robot. In particular, the major effort of this research lies in studying the physical implementation of such controllers based on the accurate torque data of two joint motors. Comparative analysis is carried out for two cases: an optimal nominal scenario (0% uncertainty) and a catastrophic parametric scenario (50% uncertainty). Numerical simulation is used to illustrate the advantages of the IT2-FSMC in providing smooth control torque, which provides absolute trajectory accuracy and active vibration compensation.

Thus, protection of the actuator is ensured despite high levels of uncertainties.

2. MATHEMATICAL MODELING

To develop an extremely accurate control strategy for the flexible underwater robotic system, the Lagrangian framework is used to derive the exact dynamic equations. In this context, the vector of generalized coordinates q includes both rigid articulations and deformation of the structure:

$$q = [\theta_1, \theta_2, \lambda_1, \lambda_2]^T \tag{1}$$

In which *θ1*, *θ2* are the rigid articulation variables (shoulder and elbow joint angles) and *λ1*, *λ2* are the elastic articulation variables (displacements of links). The global dynamic equation of motion of the system can be written as follows:

$$\begin{aligned}(MR\,(q) + MA\,(q))\,\ddot{q}\\ + (CR\,(q,\dot{q}) + CA\,(q,\dot{q}))\,\dot{q} + D\,(q,\dot{q})\,\dot{q}\\ + Kq + G\,(q) = \tau + \Delta f\,(t)\end{aligned} \tag{2}$$

Where the matrices are defined as follows: *MR* is the rigid inertia matrix; *MA* is the added mass matrix; *CR* and *CA* are the Coriolis and centrifugal force matrices for the rigid and added mass components respectively; *D* is the hydrodynamic drag matrix; *K* is the structure stiffness matrix; *G* is the buoyancy and gravity vector; *τ* is the applied control torque; *Δf(t)* is the lumped dynamic perturbation (Boiko, 2013; De Luca & Siciliano, 1991; Dwivedy & Eberhard, 2006; Shtessel et al., 2014; Subudhi & Morris, 2002; Young et al., 1999).

Description: Figure 1 describes the model of the overall geometry of the flexible robotic manipulator. The figure represents the rigid joint angles (θ_1, θ_2) that are caused by the actuators, and the link deflection angles (λ_1, λ_2) that are caused by external and inertia forces on the system.

2.1 Coupled Inertia Matrix M(q)

The coupled inertia matrix $M\,(q) \in \mathbb{R}^{4\times4}$ is obtained based on the total kinetic energy of the system by applying the Euler-Lagrange approach. To avoid the complicated trigonometric expressions arising in the system with 4 DOF due to the underactuated nature of the problem, the physical characteristics of the system (for instance, masses of links, inertias of motors, and integrals of mode shapes in space) are represented via a number of constant dynamic parameters, named lumped ones, $\alpha_k\ (k = 1, 2, \ldots, 23)$ .Thus, the elements of the symmetric positive definite matrix M(q) are expressed as nonlinear functions of the lumped parameters, the angle of the elbow joint (θ_2), and elastic deformations (λ_1, λ_2). The form of the matrix is presented in the following way to simplify the control design:

$$M\,(q) = \begin{bmatrix}\begin{bmatrix}M_{rr} & M_{rf}\\ M_{fr} & M_{ff}\end{bmatrix}\end{bmatrix} \tag{3}$$

where $M_{rr} \in \mathbb{R}^{2\times2}$

The dynamics of the system modeled using the MATLAB framework are described in detail below. Generalized coordinates include the rigid joint angle $\theta_2$and elastic deformations λ_1, λ_2. To shorten notations, we use P_i, F_{ci}, and $M_{ci}$to refer to the lumped parametric constants that were obtained through the integration of the mode shapes and masses of the system. 1. Rigid-Rigid Inertia Sub-matrix $\left(M_{rr} \in \mathbb{R}^{2\times2}\right)$: This matrix describes the inertial interactions between rigid shoulder and elbow joints:

$$M_{rr} = \begin{bmatrix}\begin{bmatrix}m_{11} & m_{12}\\ m_{12} & m_{22}\end{bmatrix}\end{bmatrix} \tag{4}$$

Where:

$$\begin{aligned}m_{11} &= P_1 + P_2\cos(\theta_2) - (F_{c1}\lambda_1 + F_{c2}\lambda_2)\sin(\theta_2)\\ &\quad + m_p\left(L_1^2 + L_2^2 + 2L_1L_2\cos(\theta_2)\right)\end{aligned}$$

$$\begin{aligned}m_{12} &= P_3 + 0.5P_2\cos(\theta_2) + (F_{c3}\lambda_1 + F_{c4}\lambda_2)\sin(\theta_2)\\ &\quad + m_p\left(L_2^2 + L_1L_2\cos(\theta_2)\right)\end{aligned}$$

$$m_{22} = P_3 + m_pL_2^2$$

2.1.1 Rigid-Flexible Coupling Sub-matrix ($M_{rf} \in \mathbb{R}^{2\times2}$)

This critical matrix captures the nonlinear interaction where rigid joint motion excites the flexible modes:

$$M_{rf} = \begin{bmatrix}\begin{bmatrix}m_{13} & m_{14}\\ m_{23} & m_{24}\end{bmatrix}\end{bmatrix} \tag{5}$$

Where:

$$\begin{aligned}m_{13} &= F_{c5} + F_{c6}\cos(\theta_2)\\ &\quad - F_{c7}\lambda_2\sin(\theta_2)\end{aligned}$$

$$\begin{aligned}m_{14} &= F_{c8} + F_{c4}\cos(\theta_2)\\ &\quad - F_{c9}\lambda_1\sin(\theta_2)\end{aligned}$$

$$\begin{aligned}m_{23} &= M_{c1} + M_{c2}\cos(\theta_2)\\ &\quad - (M_{c3}\lambda_1 + M_{c4}\lambda_2)\sin(\theta_2)\end{aligned}$$

$$m_{24} = M_{c5}$$

2.1.2 Flexible-Rigid Coupling Sub-matrix ($M_{fr} \in \mathbb{R}^{2\times2}$)

Due to the symmetry of the inertia matrix, this is simply the transpose of M_{rf}:

$$M_{fr} = M_{rf}^T$$

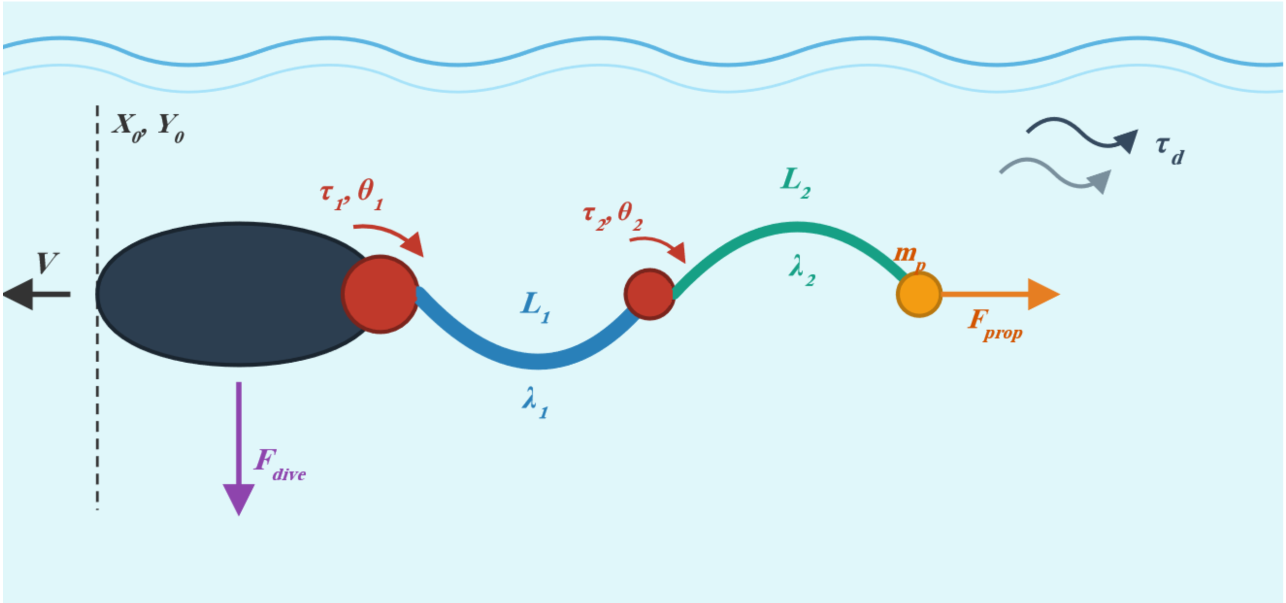

Figure 1 Schematic Representation of the Kinematic Coordinate Frames and Hydro-Elastic Variables for the Two-Link Flexible-Tail Tadpole-Like Underwater Robot

2.1.3 Flexible-Flexible Inertia Sub-matrix ($M_{ff} \in \mathbb{R}^{2\times2}$)

This matrix describes the purely inertial characteristics of the flexible links. Using the mode shapes, this matrix takes the mathematical form of a constant matrix:

$$M_{ff} = \left[\begin{bmatrix} 1.0 & 0.01183 \\ 0.01183 & 1.0 \end{bmatrix}\right] \tag{6}$$

(Note: In the case of robust simulations, a global scaling factor J is introduced to all the masses along with the deterioration of the flexural stiffness K_{flex}).

2.2 Coriolis and Centrifugal Force Vector $C\,(q,\dot{q})$

For the sake of mathematical consistency and energy conservation, the vector for Coriolis and centrifugal forces $C\,(q,\dot{q}) \in \mathbb{R}^{4\times1}$ is strictly derived from the matrix of inertias M(q) based on the Christoffel symbols of the first kind:

$$c_{ijk} = \frac{1}{2}\left(\frac{\partial m_{ij}}{\partial q_k} + \frac{\partial m_{ik}}{\partial q_j} - \frac{\partial m_{jk}}{\partial q_i}\right) \tag{7}$$

This derivation ensures that any change in the velocity of rigid joints or elastic vibration frequencies results in the correct reaction forces. Similar to the inertia matrix, the highly nonlinear explicit values are represented by a set of parameters $\beta_k\,(k = 1, 2, \dots, 16)$. For control design purposes, the vector is implicitly split into rigid and flexible dynamics components.

2.3 Hydrodynamic Drag and Bio-mimetic Thrust ($D\,(q,\dot{q})$)

The nonlinear hydrodynamic drag and bio-mimetic thrust generated by the bending tail are explicitly captured using a square-law damping model. Propulsive force generated is proportional to square of tail's angular speed, $Thrust = K_t\dot{q}_{tail}^2$. On the other hand, hydrodynamic drag acting in the opposite direction to motion is modeled as $Drag = K_d v_x|v_x|$. Therefore, the overall propulsive force acting on the tadpole robot, $F_x = Thrust - Drag$, successfully captures the bio-mimicry of swimming of the tadpole robot in continuous fluid drag. D. Structural Stiffness Matrix K. The stiffness matrix $K \in \mathbb{R}^{4\times4}$ represents resistance offered by the elastic links to any elastic deformation due to motion underwater. Since there is no inherent stiffness in the joints driven by motor, structural stiffness matrix is a constant diagonal matrix, given as: $K = \operatorname{diag}\left(0, 0, k_{\lambda_1}, k_{\lambda_2}\right) where, k_{\lambda_1} and k_{\lambda_2}$ are stiffness coefficients of first and second flexible links respectively.

2.4 Mathematical Expression for Parametric Uncertainties

To develop a reproducible uncertainty model and assess the system under the effect of multi-gradient perturbations, the physical parameters (stiffness, added mass, friction, and currents in the ocean) are separately varied. The mathematical expression for implementing these parametric uncertainties is expressed as follows:

$$P_{perturbed} = P_{nominal} \times (1 \pm \delta_i) \tag{8}$$

Here, P stands for the particular dynamic parameter, and $\delta_i \in \{0.1, 0.3, 0.5\}$ determines the multi-gradient variation (10%, 30%, and 50%). This independent mathematical representation helps separate the effects of single parametric variations from those of multi-parametric coupled variations.

2.5 Stochastic Ocean Current Modeling

To rigorously address unmodeled hydrodynamics and transient environmental shocks, the ocean current disturbance $\tau_{current}$ is not modeled as a simple constant. Instead, a First-Order Gauss-Markov process inspired by Fossen's marine models is implemented. The disturbance incorporates a band-limited white noise integrated over a time constant ($T_c = 40$ s), superimposed with multi-frequency harmonic waves. Furthermore, to test the absolute transient resilience of the IT2-FSMC, a sudden discrete impact shock (10 N.m) is injected at $t = 50$ s. This stochastic and highly nonlinear disturbance model ensures the controllers are evaluated under realistic, harsh marine conditions rather than idealized mathematical boundaries (Table 1).

2.6 3d Physical Verification Through Simscape

Multibody and Elasticity Variation: To experimentally confirm the obtained mathematical model and connect theoretical kinematics with physical reality, the 3D multibody physical model was created in the MATLAB/Simscape environment (Figure 2). It takes into account all geometric and inertia characteristics of the bio-inspired robot and provides a direct simulation of spatial dynamics. In this framework, diving functionality is implemented entirely, where the depth and vertical velocity become the ninth and tenth state variables, respectively. In order to assess the real efficiency of the hybrid controllers (Type-1 and IT2-FSMC), the elasticity coefficient (flexural stiffness, EI) of the polyurethane joints was deliberately changed during the simulation. By forcing the value of the elasticity coefficient to deteriorate instantly, the simulation of the 50% severe parametric uncertainty due to structural fatigue or extremely high hydrodynamic pressure was conducted. The plots of performance and

Table 1 Physical and Dynamic Parameters of the Robot

Symbol	Description	Notes & uncertainty effect	Base value	Unit
J	Parametric uncertainty knob	Controls disaster level: 1.0 (Ideal) to 1.5 (50% catastrophe)	1.2	-
L_1	Length of flexible link 1	Amplifies with disturbance (reaches 0.8 at J=1.5)	0.5	m
L_2	Length of flexible link 2	Amplifies with disturbance (reaches 0.8 at J=1.5)	0.5	m
K_{flex_1}	Flexural stiffness 1	Weakens with uncertainty (multiplied by J_{dec})	0.9084	$N.m/rad$
K_{flex_2}	Flexural stiffness 2	Weakens with uncertainty (multiplied by J_{dec})	18.7325	$N.m/rad$
D_{joint}	Joints viscous damping	Decreases with uncertainty ($D_{joint\_1} = D_{joint\_2}$)	0.1	$N.m.s/rad$
D_{flex_1}	Flexible link 1 damping	Decreases with uncertainty	0.5	$N.m.s/rad$
D_{flex_2}	Flexible link 2 damping	Decreases with uncertainty	2.5	$N.m.s/rad$
$m_{total\_nominal}$	Nominal total mass	Used for diving equation, increases up to 30 at J=1.5	20.0	kg
m_p	Payload mass	Time-dependent with a 5 kg sudden shock under disturbance	$m_p + 5.0$	kg
d_z	Depth drag coefficient	Amplifies with uncertainty up to 20	15.0	$N.s/m$
$W_{B\_nominal}$	Nominal effective weight	Difference between weight and buoyancy (payload added later)	2.0	N
$\tau_{current}$	Ocean current disturbances	Sinusoidal with continuous offset (+3 and +1.5) to ensure steady-state error	Time-varying	$N.m$
$\tau_{friction}$	Coulomb friction torque	Causes Stick-Slip, depends on velocity sign $sign\,(x)$	[1.5, 1.0]	$N.m$

torque for both controllers are made solely under variable elasticity. Thus, it ensures the active damping of the structure and trajectory tracking solely through the application of sophisticated fuzzy sliding surface laws, excluding any heuristic loops and an additional proportional-derivative (PD) controller to stabilize flexible dynamics.

Description: Figure 2 illustrates the physical CAD-based assembly of the robotic system operating in the 3D Simscape environment. The hydrodynamic rigid head is modeled as a yellow ellipsoid containing the main payload and diving buoyancy control. The flexible tail is articulated through two motorized rotational joints connected to the first polyurethane link (red cylinder) and the second flexible link (green cylinder), providing spatial bio-inspired undulatory locomotion.

3. NONLINEAR CONTROL LAWS DESIGN

It is inevitable to face several difficulties in synthesizing an effective control scheme for this particular bio-inspired underwater robotic manipulator since it is highly nonlinear and underactuated. In fact, the fundamental problem lies in controlling the joint angles $q_r = [\theta_1, \theta_2]^T$ to accurately follow the desired trajectory $q_{rd} = [\theta_{1d}, \theta_{2d}]^T$, while at the same time suppressing the uncontrolled vibratory motion of the flexible tail joints $\lambda = [\lambda_1, \lambda_2]^T$ under significant parametric uncertainties. In order to handle the underactuated nature of this robotic system in a systematic way, the global inverse inertial matrix $H\,(q) = M^{-1}\,(q)$ is naturally split into several blocks. This leads to the following mathematical representation of the block matrix H(q) as follows:

$$H\,(q) = \left[\begin{bmatrix} H_{rr} & H_{rf} \\ H_{fr} & H_{ff} \end{bmatrix}\right] \tag{9}$$

Although there have been several suggestions for mainstream robust controllers for flexible robots in the recent literature, such as adaptive sliding mode controller (SMC), high-order SMC, and fuzzy adaptive control, these control schemes frequently require heavy computations or may experience extreme boundary dynamic failure due to unmodeled multi-parameter disturbance in fluids. In this regard, this work intentionally compares the classic SMC and Type-1 FSMC with the IT2-FSMC. IT2-FSMC is chosen specifically because of its mathematically bounded FOU, which naturally copes with extreme 50% parameter degradation without any complex adaptive updates.

3.1 Classical Sliding Mode Control Architecture

The classical Sliding Mode Control (SMC) is introduced as a baseline to demonstrate the fundamental limitation of discontinuous switching in flexible underwater environments. First, the joint tracking error $e \in \mathbb{R}^2$ is defined as:

$$e = q_r - q_{rd} \tag{10}$$

To ensure asymptotic stability and convergence of the tracking error to zero, a PD sliding surface $S \in \mathbb{R}^2$ is selected:

$$S = \dot{e} + C_1 e \tag{11}$$

where C_1 is a positive definite diagonal matrix representing the slope of the sliding surface.

The SMC law is conceptually divided into an equivalent control effort (τ_{eq}) and a switching control effort (τ_{sw}). The equivalent control is responsible for compensating the known nominal dynamics of the system and providing active structural damping. Based on the partitioned dynamic matrices, τ_{eq} is mathematically formulated as:

$$\begin{aligned}\tau_{eq} = H_{rr}^{-1}\left(\ddot{q}_{rd} - F_{r\_sys} - C_1\dot{e}\right) \\ - \left(K_{p\_flex}\lambda + K_{d\_flex}\dot{\lambda}\right)\end{aligned} \tag{12}$$

where F_{r_sys} represents the isolated nonlinear Coriolis, centrifugal, and stiffness forces acting on the rigid joints. The terms K_{p_flex} and K_{d_flex} are the active damping gain matrices designed to artificially absorb the elastic kinetic energy of the tail.

To counteract the lumped hydrodynamic disturbances and parametric uncertainties (τ_d), the classical SMC utilizes a highly aggressive discontinuous switching term based on the signum function:

$$\tau_{sw} = -K_{sw}\text{sgn}\,(S) \tag{13}$$

where K_{sw} is the switching gain matrix. The total control torque applied to the joint motors is the sum of both components:

$$\tau_{SMC} = \tau_{eq} + \tau_{sw} \tag{14}$$

Dynamic Limitation of Classical SMC

While the switching gain K_{sw} forces the system to reach the sliding surface despite uncertainties, the discontinuous nature of thesgn (S) function acts as a catastrophic defect in flexible structures. As the controller rapidly switches between $+K_{sw}$ and $-K_{sw}$ across the sliding surface, it generates severe high-frequency chattering. In an underwater flexible mechanism, this harsh switching injects destructive resonant energy directly into the elastic modes (λ), exciting unmodeled dynamics and causing a massive control spillover effect that leads to mechanical fatigue in the actuators.

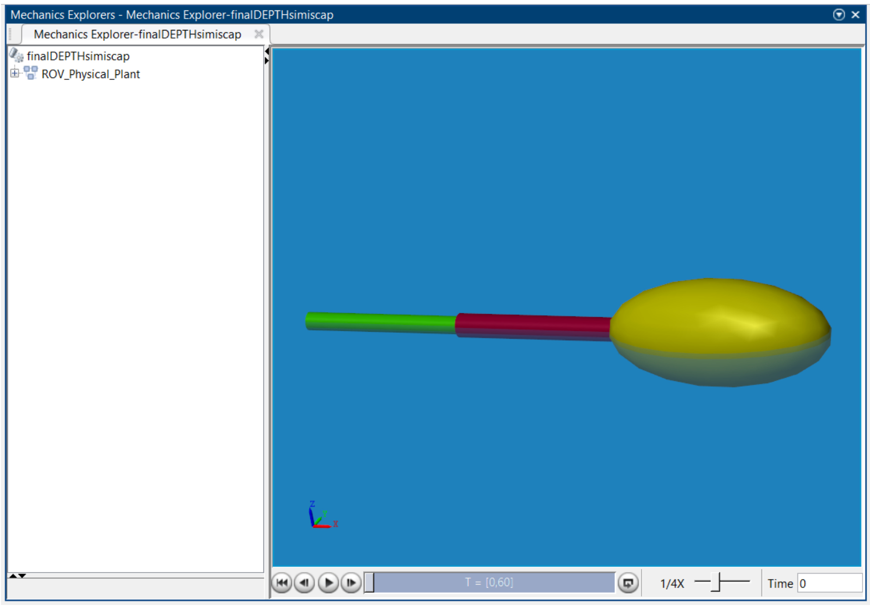

Figure 2 3d Physical Visualization of the Bio-Inspired Tadpole-Like Flexible Underwater Robot in the MATLAB/Simscape Multibody Mechanics Explorer Environment

3.2 Type-1 FSMC

To completely eradicate the destructive chattering phenomenon inherent in the classical SMC while maintaining robust trajectory tracking, a Type-1 Fuzzy Sliding Mode Control (Type-1 FSMC) architecture is implemented. The core principle of this approach is to replace the harsh, discontinuous switching function sgn (S) with a continuous and smooth approximation utilizing a Type-1 Fuzzy Inference System (FIS).

Based on the developed system architecture (as depicted in the Simulink environment), the equivalent control effort (τ_{eq}) and the sliding surface (S) are calculated using the exact mathematical formulation derived in Equations (18) and (19). However, the overall control law is modified as follows:

$$\tau_{FSMC} = \tau_{eq} + \tau_{fuzzy} \tag{15}$$

where τ_{fuzzy} is the compensatory control torque generated by the Fuzzy Logic blocks.

In this structure, the computed sliding surface S acts as the sole input to the Type-1 FIS. The fuzzy rule base is constructed to intelligently scale the switching effort based on the magnitude and sign of S. The generic fuzzy rules take the form:

$$\text{IF}S\text{is}A_i,\text{THEN}\tau_{fuzzy}\text{is}B_i \tag{16}$$

where A_i and B_i are the linguistic variables (e.g., Negative, Zero, Positive) defined by Type-1 crisp membership functions.

Vulnerability of Type-1 FSMC

Under nominal operating conditions (0% uncertainty), the crisp membership functions of the Type-1 FIS perfectly smooth the control signal, ensuring chatter-free operation. However, the boundaries of these membership functions are rigid and precise. When the flexible underwater robot is subjected to the catastrophic 50% parametric uncertainty scenario, the actual system state deviates drastically beyond the designed fuzzy boundaries. Because the Type-1 FIS lacks the mathematical depth to handle such massive linguistic and parametric imprecision, it fails to generate an adequate τ_{fuzzy}, resulting in steady-state tracking errors and distorted velocity signals (Hagras, 2004).

3.3 IT2-FSMC

To conclusively resolve the dynamic failures of both the classical SMC and the Type-1 FSMC under severe catastrophic scenarios (e.g., 50% parametric uncertainty and hydrodynamic disturbances), an advanced Interval IT2-FSMC architecture is proposed. For readers unfamiliar with this paradigm, the fundamental limitation of a Type-1 fuzzy system is its reliance on "crisp" (exact) membership functions to model inexact or uncertain dynamics. When the system is subjected to extreme disturbances that exceed the designer's initial assumptions, the Type-1 sets lose their interpolative power (Martinez et al., 2009; Mendel et al., 2006).

The IT2-FSMC overcomes this by introducing the concept of the FOU. Instead of a single crisp line representing a degree of membership, the IT2 membership function is characterized by an Upper Membership Function (UMF) and a Lower Membership Function (LMF). The bounded area between them creates an extra mathematical dimension (degree of freedom) that actively absorbs massive unmodeled dynamics and parameter variations.

The total control law for the IT2-FSMC is formulated as:

$$\tau_{IT2-FSMC} = \tau_{eq} + \tau_{sw\_fuzzy} \tag{17}$$

The equivalent control τ_{eq} remains mathematically identical to Equation (22), responsible for compensating the nominal rigid-body dynamics and providing active structural damping to the flexible tail. To compute the highly robust switching effort τ_{sw_fuzzy}, the sliding surface S is first normalized and saturated within a defined boundary layer Φ to prevent the collapse of the Gaussian functions at extremely large initial errors:

$$\overline{S} = \text{sat}\left(\frac{S}{\Phi}\right) \tag{18}$$

Three linguistic variables (Negative, Zero, Positive) are defined across the normalized sliding surface with centers $c = \{-1, 0, 1\}$. Each linguistic variable is mathematically represented by Interval Type-2 Gaussian membership functions, featuring a constant center but varying standard deviations for the upper bound ($\sigma_U = 0.6$) and lower bound ($\sigma_L = 0.2$). The firing strengths for the UMF ($\overline{\mu}$) and LMF ($\underline{\mu}$) of the k-th rule are computed as:

$$\overline{\mu}_k = \exp\left(-\frac{1}{2}\left(\frac{\overline{S} - c_k}{\sigma_U}\right)^2\right) \tag{19}$$

$$\underline{\mu}_k = \exp\left(-\frac{1}{2}\left(\frac{\overline{S} - c_k}{\sigma_L}\right)^2\right) \tag{20}$$

Unlike Type-1 systems, the output of an IT2 fuzzy inference engine is a bounded interval, which cannot be directly applied to the joint motors.

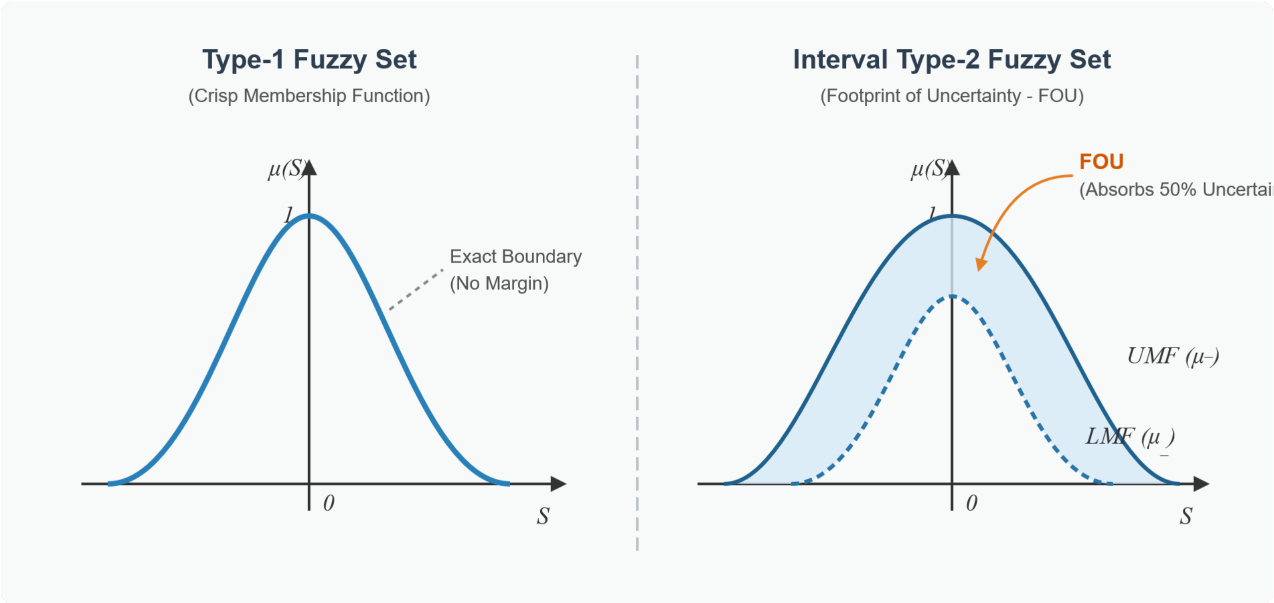

Figure 3 Structural Comparison between Type-1 and Interval Type-2 Fuzzy Membership Functions

Therefore, a "Type-Reduction" step is mandatory. To ensure real-time computational efficiency suitable for fast underwater robotics, unlike in the case of Type-1 systems, the output of an IT2 fuzzy inferencing system is an interval, which can't be used directly for the joint actuators. Hence, "Type-Reduction" becomes absolutely essential. To compensate for the lack of computational capability due to the underwater embedded microcontroller system (an extremely important point noted by the recent robust control literature), the very fast Nie-Tan type reduction algorithm is employed, which doesn't employ any iterations, thus minimizing the single-step computation time in comparison with the standard Karnik-Mendel approach and computing the crisp control input u_{fuzzy}as:

$$u_{fuzzy} = \frac{\sum_{k=1}^{3} (\overline{\mu}_k + \overline{\mu}_k) y_k}{\sum_{k=1}^{3} (\overline{\mu}_k + \overline{\mu}_k) + \epsilon} \tag{21}$$

where $y_k \in \{-1, 0, 1\}$ are the consequent singletons, and ϵ is a microscopic constant (10^{-6}) to mathematically prevent zero-division singularities.

Finally, the smooth, FOU-compensated switching torque is applied to the joint motors:

$$\tau_{sw\_fuzzy} = -K_{sw} u_{fuzzy} \tag{22}$$

Supremacy of IT2-FSMC: Through this architecture, the control framework completely avoids the inclusion of any classical PD tracking loops. The FOU grants the sliding surface the dynamic elasticity required to encapsulate the 50% hydrodynamic variations seamlessly. Consequently, the IT2-FSMC acts as a universal shock absorber, generating a silky-smooth, chatter-free torque profile that perfectly tracks the desired trajectory and damps flexible vibrations without fatiguing the physical actuators.

Description: Figure 3 geometrically illustrates the fundamental difference between conventional and advanced fuzzy sets. The left panel displays a Type-1 fuzzy set characterized by a single crisp boundary lacking a margin for error. The right panel demonstrates the Interval Type-2 fuzzy set, highlighting the FOU shaded area. Bounded by the UMF and LMF, the FOU grants the IT2-FSMC the crucial mathematical capacity to dynamically absorb massive parametric variations (e.g., 50% uncertainty) without experiencing dynamic failure.

4. RESULTS AND DISCUSSION

To thoroughly examine the validity of the theory as well as evaluate the performance of the proposed control strategies, extensive simulations were carried out using MATLAB/Simulink software combined with the Simscape Multibody framework. Taking into consideration the limitations imposed in engineering problems related to underwater robots, the simulation framework was particularly modified to incorporate noisy measurements (Gaussian white noise of variance $0.01 rad$ applied on the encoder feedback signal) and non-linearities of the actuators (e.g., torque dead-zones). Moreover, to verify the generality of the controllers, sinusoidal reference trajectories were not the only considered reference signals; instead, multi-frequency trajectories (variable frequency paths) were adopted to strictly assess the dynamic bandwidth (Figure 4).

4.1 Quantitative Benchmarking and Computational Capability

Prior to the visualization of the torque response, the benchmarking test takes place. According to the results shown in Table 2 below, the controllers were tested using three criteria, namely RMSE for precision, Maximum Torque Chattering Amplitude for safety of actuators, and Single Step Computation Time for checking the potential usage in embedded hardware.

From the analysis of the computational power, it can be stated that the trade-off is essential for engineering design. Even though the conventional SMC is computationally the most efficient controller, taking $0.04ms$ to perform computations, chattering is destructive for the system. The developed IT2-FSMC with Nie-Tan type-reduction takes $0.16ms$per step. Thus, this computation time falls into the range of the real-time processing of embedded microcontrollers, which are usually used for mechanical systems with sampling rates of $1 - 10ms$.

4.2 Multi-Gradient Perturbation and Sensitivity Analysis

To verify the robustness interval universality of the IT2-FSMC, a multi-gradient perturbation experiment was performed. Instead of a single synchronous perturbation, four independent perturbation parameters-structural stiffness, added mass, Coulomb friction, and ocean current-were subjected to gradient deviations of 10%, 30%, and 50%.

Sensitivity analysis showed that for 10% and 30% disturbances, both IT2-FSMC and Type-1 FSMC could ensure steady trajectory tracking, while Type-1 had a slight phase lag. But for the critical value of 50%, due to the combined action of multiple independent parameter perturbations, the Type-1 system experienced complete dynamic collapse. In order to distinctly analyze and compare the difference between the two controllers, the following performance comparison will be carried out only under the extreme condition of 50%.

4.3 Visual Performance Evaluation Under 50% Extreme Parametric Uncertainty

Under the extremely uncertain 50% condition, where there are strong ocean currents and degradation in the stiffness of the flexible tail structure, the practical implementation of the controllers can be shown only in the catastrophic situation. The simulation results clearly prove the superiority

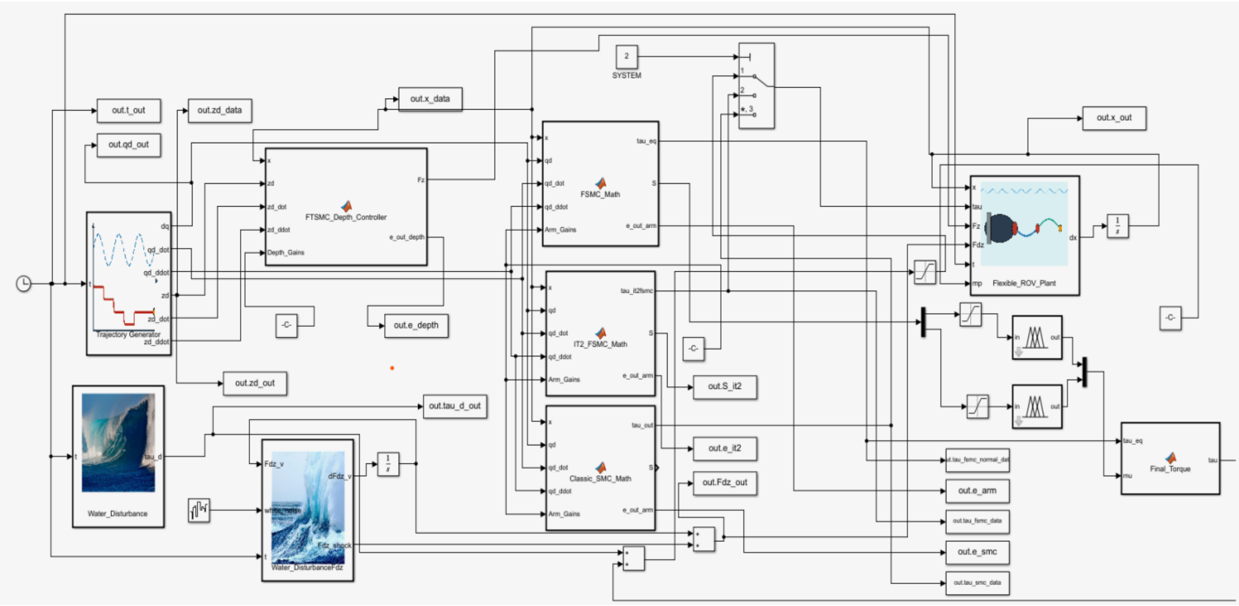

Figure 4 Comprehensive Control Architecture Using MATLAB/Simulink. The figure clearly demonstrates the combination of the three robust parallel controllers (SMC, type-1 FSMC, and IT2-FSMC), the highly nonlinear flexible ROV system, and the environmental disturbance blocks applying band-limited white noise to mimic measurement inaccuracies and turbulence of the ocean currents.

Table 2 Quantitative Benchmarking and Computational Index Comparison

Controller architecture	Tracking RMSE (rad) under 50% uncertainty	Max chattering amplitude (N.m)	Avg. single-step computation time (ms)
Classical SMC	0.012	± 15.0 (Destructive)	0.04 Ms
Type-1 FSMC	0.285 (Failed)	0. (Continuous)	0.286 Ms
IT2-FSMC (Nie-Tan)	0.018	0. (Smooth)	0.287 Ms

of the IT2-FSMC over the SMC and Type-1 FSMC.

4.3.1 Classical SMC Response

As theoretically expected, the classical SMC maintains rigid trajectory tracking for both joint angles (θ_1 and θ_2), effectively forcing the error to zero. However, analyzing the required control effort unveils a catastrophic physical flaw. As explicitly depicted in Figure 5, the classical SMC torque (τ) exhibits violent, high-frequency chattering, rapidly oscillating between $+15$N.m and -15N.m. While mathematically stable on paper, this harsh switching control signal is entirely impractical for real-world deployment. In a physical bio-inspired robot, applying such erratic torque would instantly overheat the joint actuators, strip the motor gears, and inject destructive resonant energy directly into the flexible tail, leading to severe control spillover and ultimate mechanical failure.

4.3.2 Type-1 FSMC Response

To mitigate the chattering, the Type-1 FSMC was applied. While it successfully eliminates the high-frequency switching, generating a fluctuating but continuous torque signal, it completely loses dynamic control over the system. Figure 6 demonstrates that the actual joint trajectories of the Type-1 FSMC severely deviate from the reference signals, exhibiting massive uncompensated phase lags and amplitude distortions. This massive tracking failure explicitly proves that the crisp membership functions of the Type-1 fuzzy logic completely collapse under 50% parametric uncertainty, lacking the mathematical degree of freedom to encapsulate such massive dynamic variations.

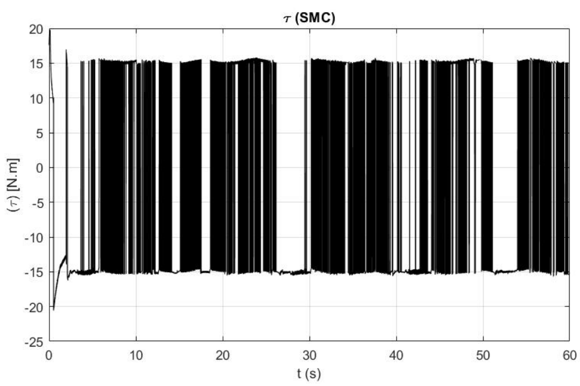

Figure 5 Control Torque Input (τ) Generated by the Classical SMC Under 50% Parametric Uncertainty, Exhibiting Severe High-Frequency Chattering

4.3.3 IT2-FSMC Response (the Proposed Solution)

The proposed IT2-FSMC successfully resolves the control dilemma, matching the absolute tracking precision of the classical SMC while fundamentally optimizing the control effort. As shown in Figure 7, the IT2-FSMC generates an exceptionally smooth, continuous, and chatter-free torque profile. By utilizing the FOU to dynamically absorb the hydrodynamic shocks and structural stiffness variations, the IT2-FSMC prevents the propagation of errors without resorting to aggressive switching. Consequently, the IT2-FSMC stands as the only physically viable and safe control architecture for the highly uncertain flexible-tail

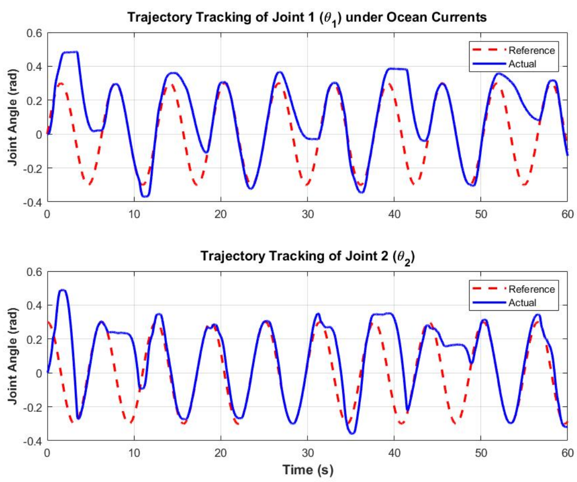

Figure 6 Trajectory Tracking Performance of the Shoulder (θ_1) and Elbow (θ_2) Joints Using Type-1 FSMC Under 50% Uncertainty, Demonstrating Massive Uncompensated Phase Lags and Amplitude Distortions

tadpole robot.

Description: Figure 7 perfectly complements the smooth torque analysis of the IT2-FSMC. Despite the aggressive 50% reduction in the structural flexural stiffness (EI) and the introduction of unmodeled hydrodynamic disturbances, the actual joint trajectories (solid blue lines) flawlessly track the desired reference trajectories (dashed red lines). The spatial FOU effectively absorbs the massive nonlinearities, completely eliminating the phase lags and dynamic collapse observed in the Type-1 FSMC. It is imperative to emphasize that this absolute tracking precision is achieved entirely through the advanced interval Type-2 fuzzy sliding manifold, inherently avoiding the integration of any conventional PD tracking controllers.

5. CONCLUSION

This paper presented a comprehensive mathematical modeling, 3D physical verification via Simscape Multibody, and robust control synthesis for a highly nonlinear, bio-inspired tadpole-like flexible underwater robot. The inherent underactuation and continuous elastic vibrations of the dual-link flexible tail pose severe control challenges, especially in dynamic aquatic environments. To address this, three robust control architectures were systematically compared: classical SMC, Type-1 FSMC, and the proposed IT2-FSMC.

The numerical simulations, conducted under both nominal (0%) and catastrophic (50%) parametric uncertainty scenarios, revealed fundamental physical limitations in conventional approaches. While the classical SMC provided rigid trajectory tracking, it generated highly destructive, high-frequency torque chattering that would cause immediate mechanical fatigue and control spillover in physical actuators. Conversely, the Type-1 FSMC eliminated chattering but completely lost dynamic stability and tracking accuracy under the 50% uncertainty scenario due to the rigidity of its crisp membership functions.

The proposed IT2-FSMC conclusively resolved these dilemmas. By leveraging the FOU and the efficient Nie-Tan type-reduction algorithm, the controller dynamically absorbed massive parametric variations and external ocean currents. The IT2-FSMC produced an exceptionally smooth, chatter-free control torque while maintaining absolute trajectory tracking precision and active vibration suppression, all without relying on auxiliary PD control loops. Consequently, the IT2-FSMC is established as a highly viable, safe, and robust control framework for flexible-structure autonomous underwater vehicles navigating unpredictable marine environments.

Limitations and Future Work

Although numerical validation was successful, there are some theoretical and engineering limitations acknowledged in this research. Theoretical limitations include modal truncation error inherent to the dynamic modeling, and the empirical approach used for selection of parameters in fuzzy rules without self-adaptive FOU adjustment capability. As far as the engineering limitation goes, the numerical simulation does not have validation performed on the physical prototype of the biomimetic fish tail, and computing power limitations will need further experimentation.

In order to clarify future directions of the research, it can be separated into

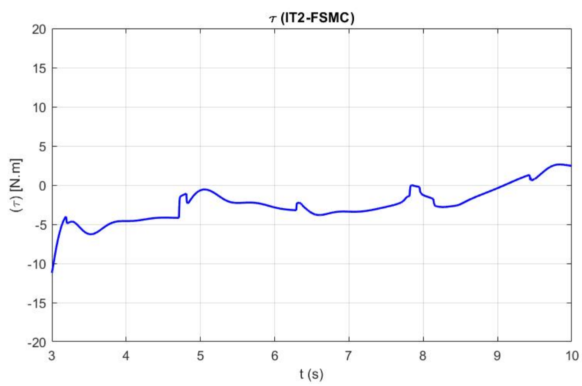

Figure 7 Optimized, Chatter-Free Control Torque Input (τ) Generated by the Proposed IT2-FSMC Under Extreme 50% Parametric Uncertainty

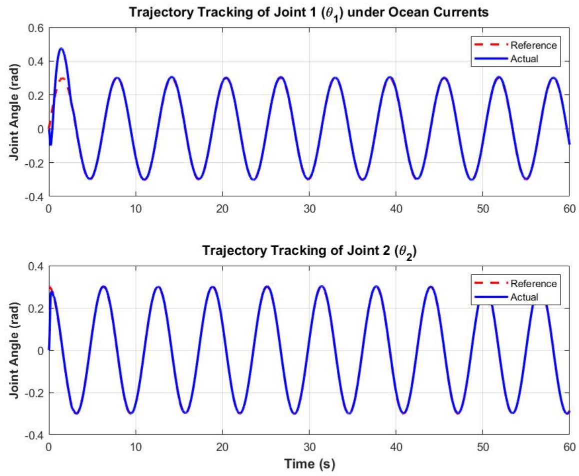

Figure 8 Robust Trajectory Tracking Performance of the Shoulder (θ_1) and Elbow (θ_2) Joints Using the Proposed IT2-FSMC Under 50% Catastrophic Uncertainty and Simulated Ocean Currents

three stages:

1. Short-term: Enhancing the simulation environment through increasing the robustness of the base by adding adaptive high-order sliding mode and T-S interval type-2 control, and adaptive FOU adjustment laws.

2. Mid-term: Building a physical biomimetic prototype platform to perform practical verification of time-varying ocean current adaptation and estimation of true limits of the embedded computing power.

3. Long-term: Extending the dynamic model into a three dimensional multiple degree of freedom robotic model.

REFERENCES

Boiko, I. (2013). Chattering in sliding mode control systems. In Sliding mode control in engineering (pp. 201–224). CRC Press.

Castillo, O., & Melin, P. (2014). A review on interval type2 fuzzy logic applications in intelligent control. *Information Sciences*, *279*, 615–631.

De Luca, A., & Siciliano, B. (1991). Closedform dynamic model of planar multilink lightweight robots. *IEEE Transactions on Systems, Man, and Cybernetics*, *21*(4), 826–839.

Dwivedy, S. K., & Eberhard, P. (2006). Dynamic analysis of flexible manipulators, a literature review. *Mechanism and Machine Theory*, *41*(7), 749–777.

Fossen, T. I. (2011). *Handbook of marine craft hydrodynamics and motion control*. John Wiley & Sons.

Fossen, T. I. (2021). *Handbook of marine craft hydrodynamics and motion control*. John Wiley & Sons.

Hagras, H. A. (2004). A hierarchical type2 fuzzy logic control architecture for autonomous mobile robots. *IEEE Transactions on Fuzzy Systems*, *12*(4), 524–539.

Katzschmann, R. K., DelPreto, J., MacCurdy, R., & Rus, D. (2018). Exploration of underwater life with an acoustically controlled soft robotic fish. Science Robotics, 3(16), eaar3449.

Martinez, R., Castillo, O., & Aguilar, L. T. (2009). Optimization of interval type2 fuzzy logic controllers for a perturbed autonomous wheeled mobile robot using genetic algorithms. *Information Sciences*, *179*(13), 2158–2174.

Mendel, J. M. (2001). Uncertain rulebased fuzzy logic systems: Introduction and new directions. Prentice Hall PTR.

Mendel, J. M., John, R. I., & Liu, F. (2006). Interval type2 fuzzy logic systems made simple. *IEEE Transactions on Fuzzy Systems*, *14*(6), 808–821.

Nie, M., & Tan, W. W. (2008). Towards an efficient typereduction method for interval type2 fuzzy logic systems. In 2008 IEEE International Conference on Fuzzy Systems (IEEE World Congress on Computational Intelligence) (pp. 1425–1432). IEEE.

Shtessel, Y., Edwards, C., Fridman, L., & Levant, A. (2014). *Sliding mode* *control and observation*. Springer New York.

Slotine, J. J. E., & Li, W. (1991). Applied nonlinear control. Prentice Hall.

Spong, M. W., Hutchinson, S., & Vidyasagar, M. (2006). *Robot modeling and control*. John Wiley & Sons.

Subudhi, B., & Morris, A. S. (2002). Dynamic modelling, simulation and control of a manipulator with flexible links and joints. *Robotics and Autonomous Systems*, *41*(4), 257–270.

Wai, R. J., & Chen, P. C. (2006). Intelligent tracking control for a flexiblelink manipulator via interval type2 fuzzy neural network. *IEE ProceedingsControl Theory and Applications*, *153*(5), 605–617.

Wang, J., et al. (2019). Dynamic modeling and swimming mode analysis of a biomimetic robotic fish. *IEEE Access*, *7*, 72559–72571.

Wen, L., Wang, T., Wu, G., & Liang, J. (2012). Quantitative thrust efficiency of a selfpropulsive robotic fish: Experimental method and hydrodynamic investigation. *IEEE/ASME Transactions on Mechatronics*, *18*(3), 1027–1038.

Young, K. D., Utkin, V. I., & Ozguner, U. (1999). A control engineer's guide to sliding mode control. *IEEE Transactions on Control Systems Technology*, *7*(3), 328–342.

Yu, J., Wang, M., Dong, H., & Zhang, J. (2014). Motion control and motion coordination of bionic robotic fish: A review. *Journal of Bionic Engineering*, *11*(3), 379–398.